Proton and neutron electromagnetic charge radii and magnetic moments from $N_f = 2 + 1$ lattice QCD

Miguel Salg, Dalibor Djukanovic, Georg von Hippel, Harvey B. Meyer, Konstantin Ottnad, Hartmut Wittig

LATTICE 2023, August 1, 2023

Outline

Motivation

- Internal structure of the nucleon still an open research field in subatomic physics
- In particular, there is a discrepancy between different determinations of the electric and magnetic charge radii of the proton
- Electromagnetic form factors of the proton and neutron of high interest

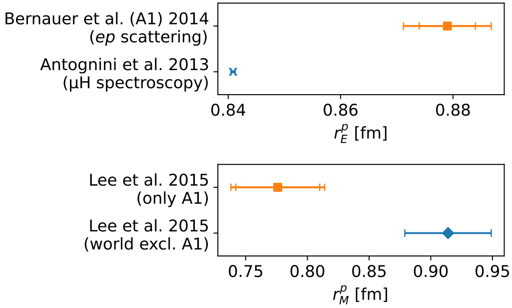

- Full calculation of the proton and neutron form factors from first principles necessitates explicit treatment of the numerically challenging quark-disconnected contributions
- Not included in many previous lattice studies

Outline

Ensembles

Coordinated Lattice Simulations (CLS)[1]

- Non-perturbatively $\mathcal{O}(a)$-improved Wilson fermions, $N_f = 2 + 1$
- $\mathrm{tr}\, M_q = 2m_l + m_s =$ const.
- Tree-level improved Lüscher-Weisz gauge action
- $\mathcal{O}(a)$-improved conserved vector current

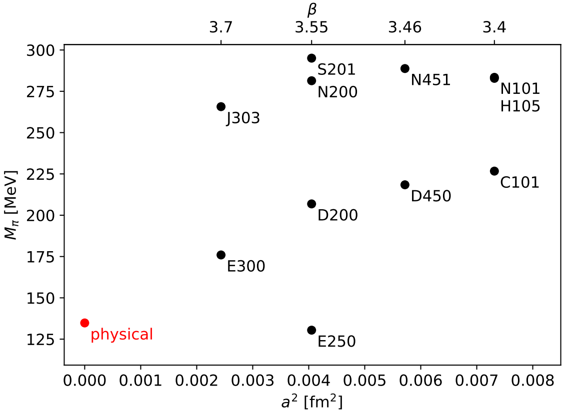

Figure: Overview of the ensembles used in this study

[1] Bruno et al. 2015; Bruno, Korzec, and Schaefer 2017.

Nucleon two- and three-point correlation functions

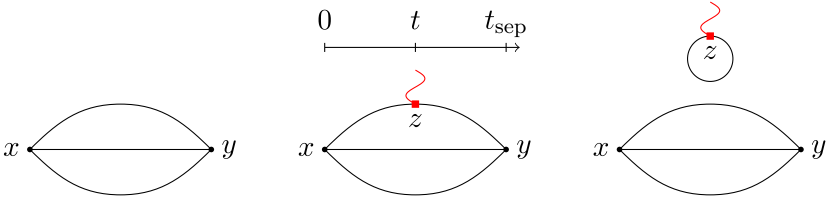

C_2 C_3^{conn} C_3^{disc}

- Measure the two- and three-point correlation functions of the nucleon
- For three-point functions, Wick contractions yield connected and disconnected contribution
- Compute the quark loops via a stochastic estimation using a frequency-splitting technique[2]
- Extract the effective form factors $G_{E,M}^{\text{eff}}$ using the ratio method[3]

[2]Giusti et al. 2019; Cè et al. 2022; [3]Korzec et al. 2009.

Excited-state analysis

- Apply summation method with varying starting values $t_{\mathrm{sep}}^{\mathrm{min}}$ for the linear fit
- Perform a weighted average over $t_{\mathrm{sep}}^{\mathrm{min}}$, where the weights are given by a smooth window function[4]

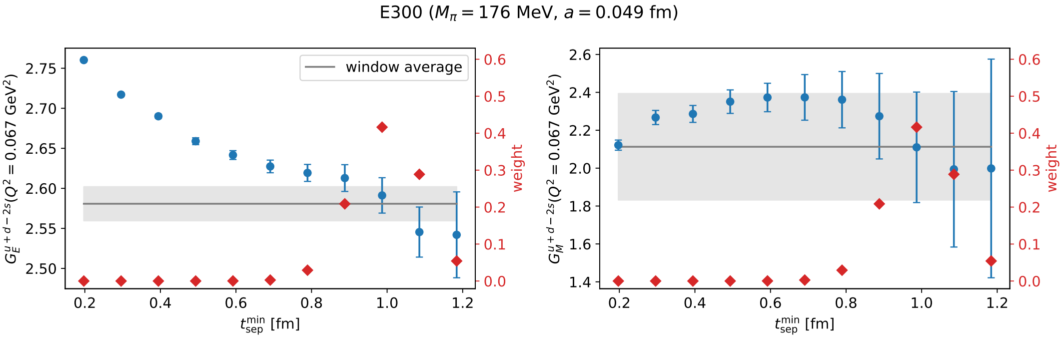

[4]Djukanovic et al. 2022; Agadjanov et al. 2023.

Excited-state analysis

D450 ($M_\pi = 218$ MeV, $a = 0.076$ fm)

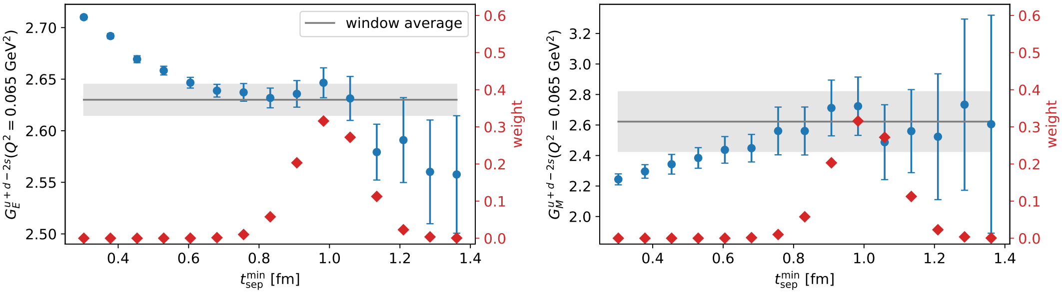

- Reliable detection of the plateau with reduced human bias (same window on all ensembles)
- Conservative error estimate

Outline

Direct Baryon χPT fits

- Combine parametrization of the Q^2-dependence with the chiral, continuum, and infinite-volume extrapolation
- Simultaneous fit of the pion-mass, Q^2-, lattice-spacing, and finite-volume dependence of the form factors to the expressions resulting from covariant chiral perturbation theory[5]
- Include contributions from the ρ (ω and ϕ) mesons in the isovector (isoscalar) channel
- Reconstruct proton and neutron observables from separate fits to the isovector and isoscalar form factors
- Perform fits with various cuts in M_π and Q^2, as well as with different models for the lattice-spacing and finite-volume dependence, in order to estimate systematic uncertainties
- Large number of degrees of freedom $\Rightarrow$ improved stability against lowering the Q^2-cut

[5] Bauer, Bernauer, and Scherer 2012.

Q^2-dependence of the isovector form factors on E300

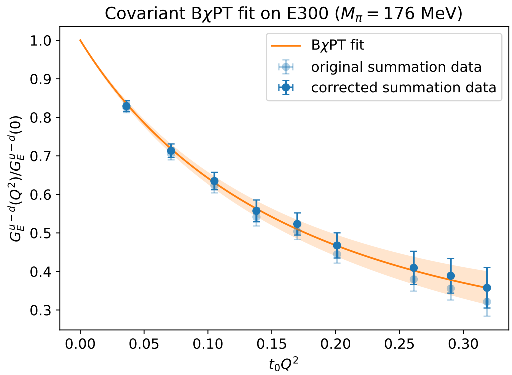

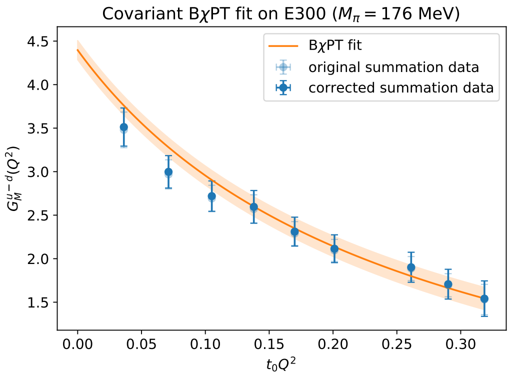

- Direct BχPT fit describes data very well
- Reduced error due to the inclusion of several ensembles in one fit

Q^2-dependence of the isoscalar form factors on E300

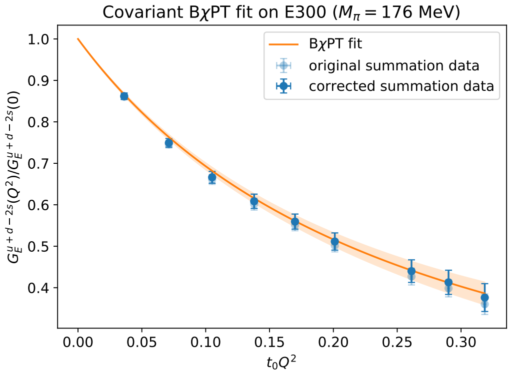

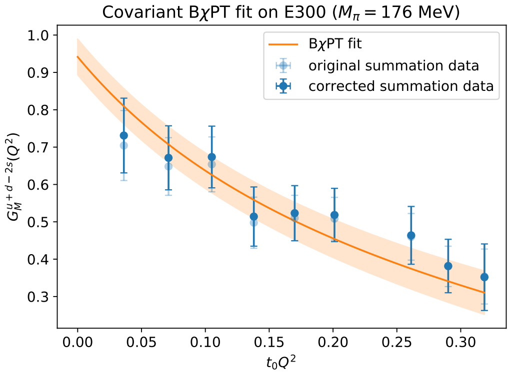

Outline

Model average

- Perform a weighted average over the results of all fit variations, using weights derived from the Akaike Information Criterion[6],

$$w_i = \exp\left(-\frac{1}{2}\mathrm{BAIC}_i\right) \Bigg/ \sum_j \exp\left(-\frac{1}{2}\mathrm{BAIC}_j\right), \quad \mathrm{BAIC}_i = \chi^2_{\mathrm{noaug,min},i} + 2n_{f,i} + 2n_{c,i}, \tag{1}$$

  where n_f is the number of fit parameters and n_c the number of cut data points
- Strongly prefers fits with low n_c, *i.e.*, the least stringent cut in Q^2 $\Rightarrow$ apply a flat weight over the different Q^2-cuts to ensure strong influence of our low-momentum data
- Determine the final cumulative distribution function (CDF) from the weighted sum of the bootstrap distributions[7]
- Quote median of this CDF together with the central $68\,\%$ percentiles

[6] Akaike 1973, 1974; Neil and Sitison 2022; [7] Borsányi et al. 2021.

Model-averaged proton form factors at the physical point

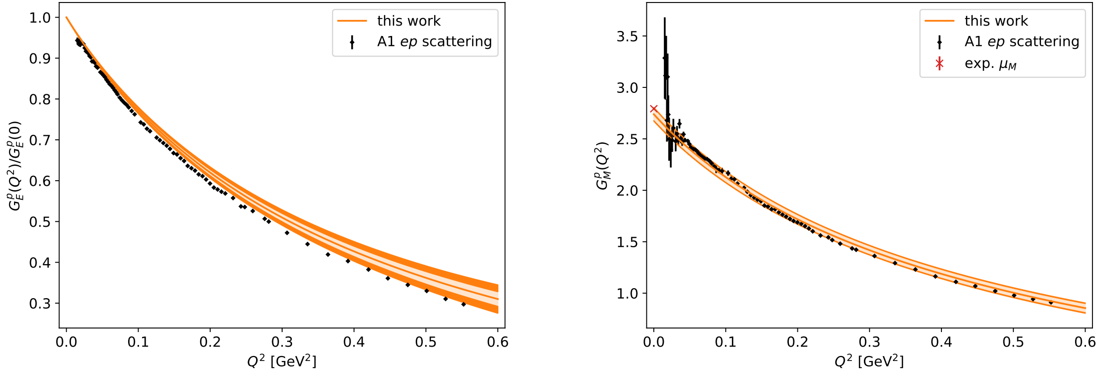

- Slightly different slope of the electric form factor compared to that of A1[8]
- Good agreement for the magnetic form factor

[8] Bernauer et al. 2014.

Model-averaged neutron form factors at the physical point

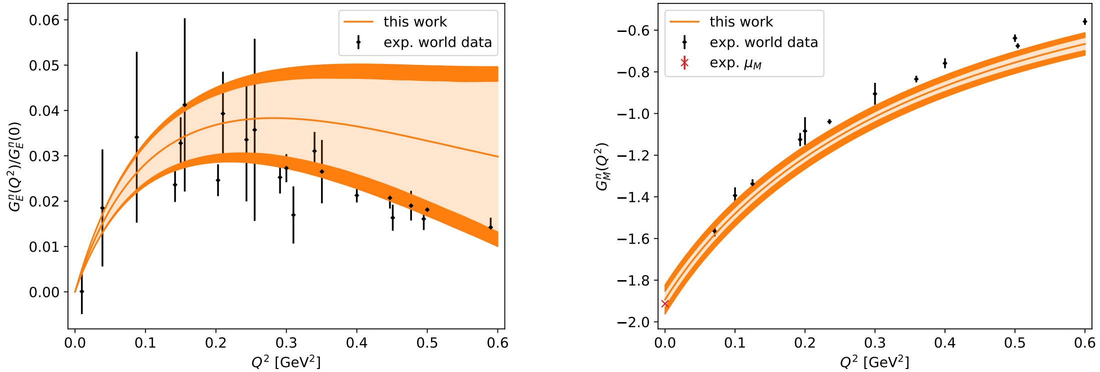

(Mostly) compatible with the collected experimental world data[9] within our errors

[9] Ye et al. 2018.

Electromagnetic charge radii and magnetic moments

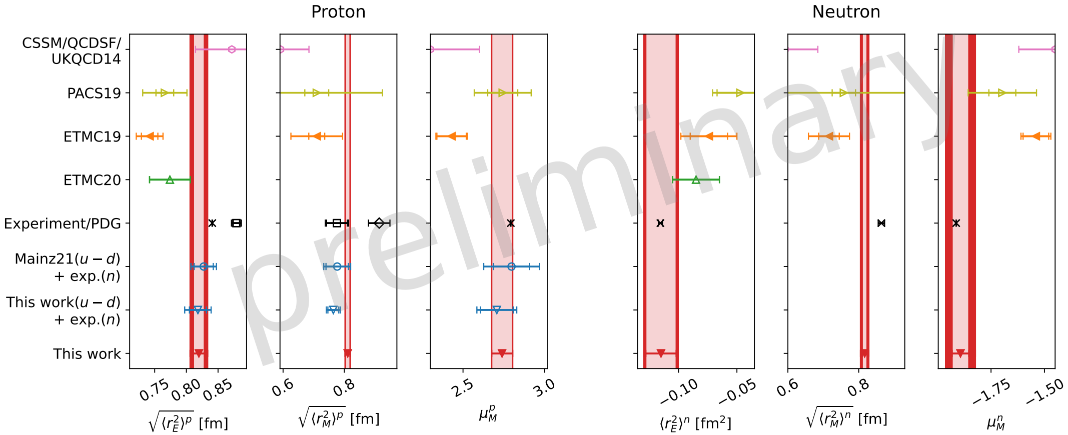

Magnetic moments reproduced, low value for $\sqrt{\langle r_E^2\rangle^p}$ clearly favored, $\sqrt{\langle r_M^2\rangle^p}$ agrees with A1

Outline

Hyperfine splitting and the Zemach radius

- Determination of nuclear properties from atomic physics
- Magnetic spin-spin interaction between the nucleus and the orbiting lepton gives rise to the hyperfine splitting (HFS)
- Electromagnetic structure of the proton influences the HFS of the s-state of hydrogen
- Relevant parameter deduced from the HFS: Zemach radius[10],

$$r_Z^p = -\frac{4}{\pi}\int_0^\infty \frac{dQ}{Q^2}\left(\frac{G_E^p(Q^2)G_M^p(Q^2)}{\mu_M^p} - 1\right) = -\frac{2}{\pi}\int_0^\infty \frac{dQ^2}{(Q^2)^{3/2}}\left(\frac{G_E^p(Q^2)G_M^p(Q^2)}{\mu_M^p} - 1\right) \tag{2}$$

- BχPT only trustworthy up to $Q^2 \approx 0.6\,\mathrm{GeV}^2$
- Tail of the integrand suppressed[11]: contribution of the form factors above $0.6\,\mathrm{GeV}^2$ to r_Z only about $1\,\%$

---

[10] Zemach 1956; [11] Lepage and Brodsky 1980

Zemach radius from the lattice

- Extrapolate BχPT fit using a z-expansion[12] *ansatz*
- Low value for r_Z^p favored
- Our estimate is not independent from the electromagnetic charge radii (based on the same form factor data)
- Large positive correlation between $\sqrt{\langle r_E^2 \rangle^p}$ and r_Z^p[13]
- Low result for r_Z^p expected, no independent puzzle

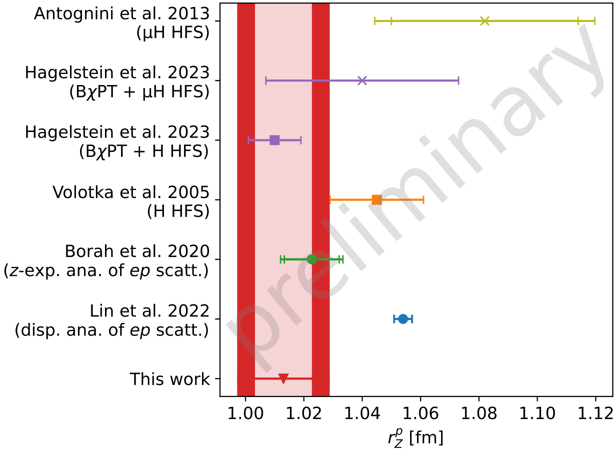

[12] Hill and Paz 2010; Lee, Arrington, and Hill 2015; [13] Friar and Sick 2005

Outline

Conclusions

- Direct determination of the electromagnetic form factors of the proton and neutron from lattice QCD including all relevant contributions
- Chiral, continuum, and infinite-volume extrapolation via matching with the predictions from covariant baryon chiral perturbation theory
- Magnetic moments of the proton and neutron agree well with the experimental values
- Small electric *and* magnetic charge radii of the proton favored
- Competitive errors, in particular for the magnetic charge radii
- Initial study of the Zemach radius works well and yields a plausible result
- Djukanovic et al. 2023 (in preparation)

Backup slides

Vector current

- Use the conserved vector current,

$$V_\mu^c(n) = \frac{1}{2}\Big(\bar\psi(n+\hat\mu a)(\mathbb{1}+\gamma_\mu)U_\mu^\dagger(n)\psi(n) - \bar\psi(n)(\mathbb{1}-\gamma_\mu)U_\mu(n)\psi(n+\hat\mu a)\Big)\,, \qquad (3)$$

or, more precisely, the symmetrized version

$$V_\mu^{cs}(n) = \frac{1}{2}\left(V_\mu^c(n) + V_\mu^c(n-\hat\mu a)\right) \qquad (4)$$

- Perform $\mathcal{O}(a)$-improvement[14]
- No renormalization required

[14] Gérardin, Harris, and Meyer 2019.

From correlation functions to form factors

- Average over the forward- and backward-propagating nucleon and over x-, y-, and z-polarization for the disconnected part
- Calculate the ratios[15]

$$R_{V_\mu}(\mathbf{q}; t_{\mathrm{sep}}, t) = \frac{C_{3,V_\mu}(\mathbf{q}; t_{\mathrm{sep}}, t)}{C_2(\mathbf{0}; t_{\mathrm{sep}})} \sqrt{\frac{\bar{C}_2(\mathfrak{q}; t_{\mathrm{sep}} - t) C_2(\mathbf{0}; t) C_2(\mathbf{0}; t_{\mathrm{sep}})}{C_2(\mathbf{0}; t_{\mathrm{sep}} - t) \bar{C}_2(\mathfrak{q}; t) \bar{C}_2(\mathfrak{q}; t_{\mathrm{sep}})}}, \tag{5}$$

where $t_{\mathrm{sep}} = y_0 - x_0$, $t = z_0 - x_0$, and $\bar{C}_2(\mathfrak{q}; t_{\mathrm{sep}}) = \sum_{\tilde{\mathbf{q}} \in \mathfrak{q}} C_2(\tilde{\mathbf{q}}; t_{\mathrm{sep}}) \Big/ \sum_{\tilde{\mathbf{q}} \in \mathfrak{q}} 1$

- At zero sink momentum, the effective form factors can be computed from the ratios as

$$G_E^{\mathrm{eff}}(Q^2; t_{\mathrm{sep}}, t) = \sqrt{\frac{2E_{\mathbf{q}}}{m + E_{\mathbf{q}}}} R_{V_0}(\mathbf{q}; t_{\mathrm{sep}}, t), \tag{6}$$

$$G_M^{\mathrm{eff}}(Q^2; t_{\mathrm{sep}}, t) = \sqrt{2E_{\mathbf{q}}(m + E_{\mathbf{q}})} \frac{\sum_{j,k} \epsilon_{ijk} q_k \operatorname{Re} R_{V_j}^{\Gamma_i}(\mathbf{q}; t_{\mathrm{sep}}, t)}{\sum_{j \neq i} q_j^2} \tag{7}$$

Excited-state analysis

- Sum the effective form factors over the operator insertion time,

$$S_{E,M}(Q^2;t_\mathrm{sep}) = \sum_{t=t_\mathrm{skip}}^{t_\mathrm{sep}-t_\mathrm{skip}} G^\mathrm{eff}_{E,M}(Q^2;t,t_\mathrm{sep}), \quad t_\mathrm{skip} = 2a \tag{8}$$

- For $t_\mathrm{sep} \to \infty$, the slope as a function of t_sep is given by the ground-state form factor,

$$S_{E,M}(Q^2;t_\mathrm{sep}) \xrightarrow{t_\mathrm{sep}\to\infty} C_{E,M}(Q^2) + \frac{1}{a}(t_\mathrm{sep} + a - 2t_\mathrm{skip}) G_{E,M}(Q^2) \tag{9}$$

- Perform a weighted average over $t_\mathrm{sep}^\mathrm{min}$, where the weights are given by a smooth window function,

$$\hat{G} = \frac{\sum_i w_i G_i}{\sum_i w_i}, \qquad w_i = \tanh \frac{t_i - t_w^\mathrm{low}}{\Delta t_w} - \tanh \frac{t_i - t_w^\mathrm{up}}{\Delta t_w}, \tag{10}$$

  where t_i is the value of $t_\mathrm{sep}^\mathrm{min}$ in the i-th fit, $t_w^\mathrm{low} = 0.9$ fm, $t_w^\mathrm{up} = 1.1$ fm and $\Delta t_w = 0.08$ fm

Q^2-dependence of the isovector form factors on E250

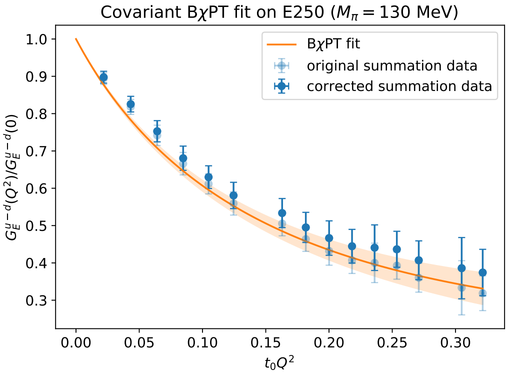

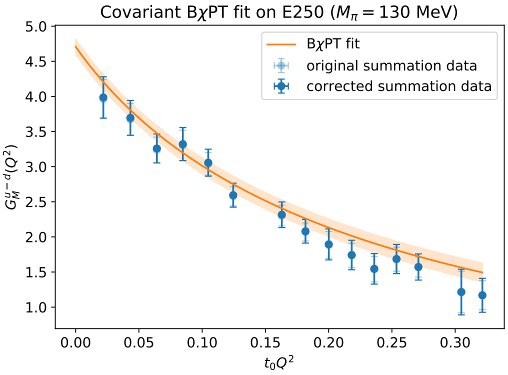

Q^2-dependence of the isoscalar form factors on E250

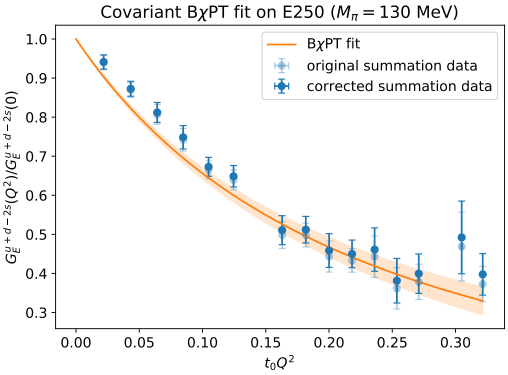

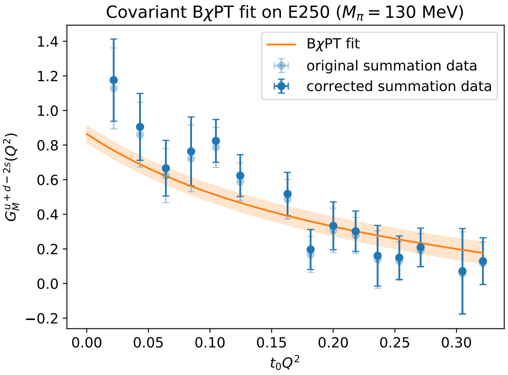

Residuals of the BχPT fits

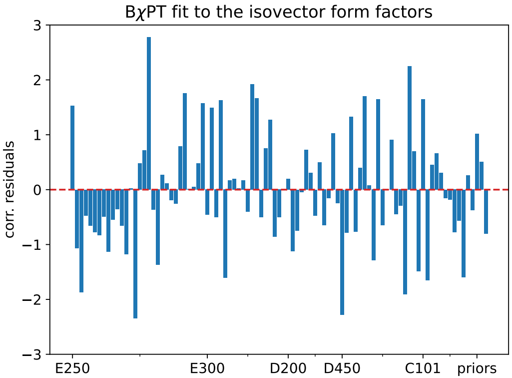

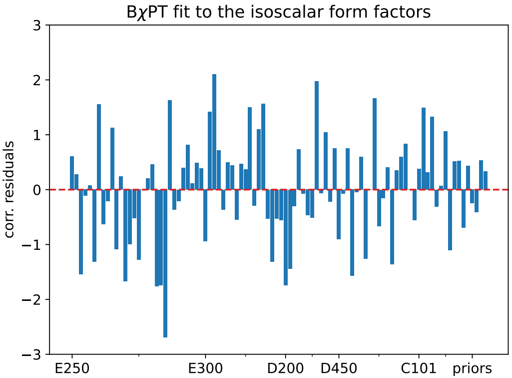

Histograms

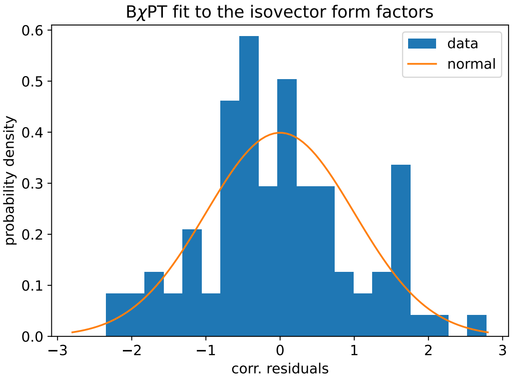

BχPT fit to the isovector form factors
data
normal
probability density
corr. residuals
0.0
0.1
0.2
0.3
0.4
0.5
0.6
−3
−2
−1
0
1
2
3

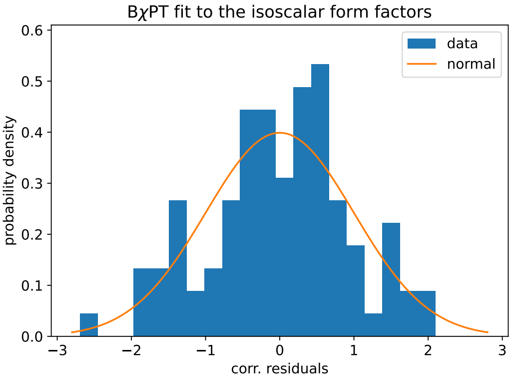

BχPT fit to the isoscalar form factors
data
normal
probability density
corr. residuals
0.0
0.1
0.2
0.3
0.4
0.5
0.6
−3
−2
−1
0
1
2
3

Q-Q plots

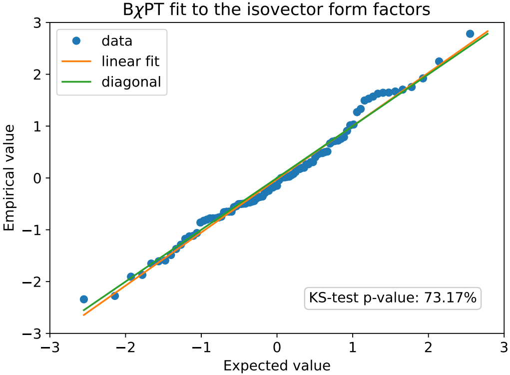

BχPT fit to the isovector form factors
data
linear fit
diagonal
KS-test p-value: 73.17%
Empirical value
Expected value
3
2
1
0
−1
−2
−3

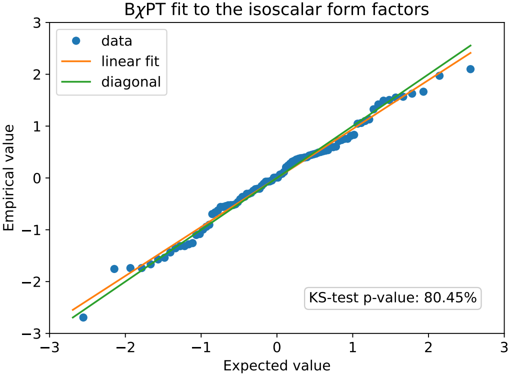

BχPT fit to the isoscalar form factors
data
linear fit
diagonal
KS-test p-value: 80.45%
Empirical value
Expected value
3
2
1
0
−1
−2
−3

Disambiguating the statistical and systematic uncertainties

- Scale the statistical variances of the individual fit results by a factor of $\lambda = 2$
- Repeat the model averaging procedure
- Assumptions:
  - Above rescaling only affects the statistical error of the averaged result
  - Statistical and systematic errors add in quadrature
- Contributions of the statistical and systematic errors to the total error,

$$\sigma_{\text{stat}}^2 = \frac{\sigma_{\text{scaled}}^2 - \sigma_{\text{orig}}^2}{\lambda - 1}, \qquad \sigma_{\text{syst}}^2 = \frac{\lambda\sigma_{\text{orig}}^2 - \sigma_{\text{scaled}}^2}{\lambda - 1} \tag{11}$$

- Consistency check: results are almost independent of λ (if it is chosen not too small)

CDFs of the EM charge radii and magnetic moment of the proton

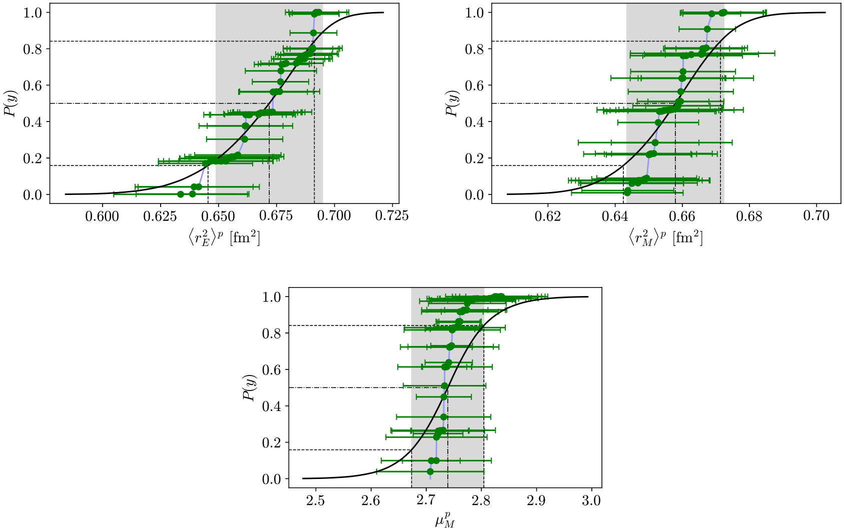

z-expansion

- Model-independent description of the Q^2-dependence of the form factors
- Map domain of analyticity of the form factors onto the unit circle,

$$z(Q^2) = \frac{\sqrt{\tau_{\text{cut}} + Q^2} - \sqrt{\tau_{\text{cut}} - \tau_0}}{\sqrt{\tau_{\text{cut}} + Q^2} + \sqrt{\tau_{\text{cut}} - \tau_0}}, \tag{12}$$

  where $\tau_{\text{cut}} = 4M_\pi^2$, and we employ $\tau_0 = 0$
- Expand the form factors as

$$\frac{G_E(Q^2)}{G_E(0)} = \sum_{k=0}^{n} a_k z(Q^2)^k, \quad G_M(Q^2) = \sum_{k=0}^{n} b_k z(Q^2)^k \tag{13}$$

- Fix $G_E(0) = a_0 = 1$

Crosscheck of direct fits with z-expansion: proton EM charge radii

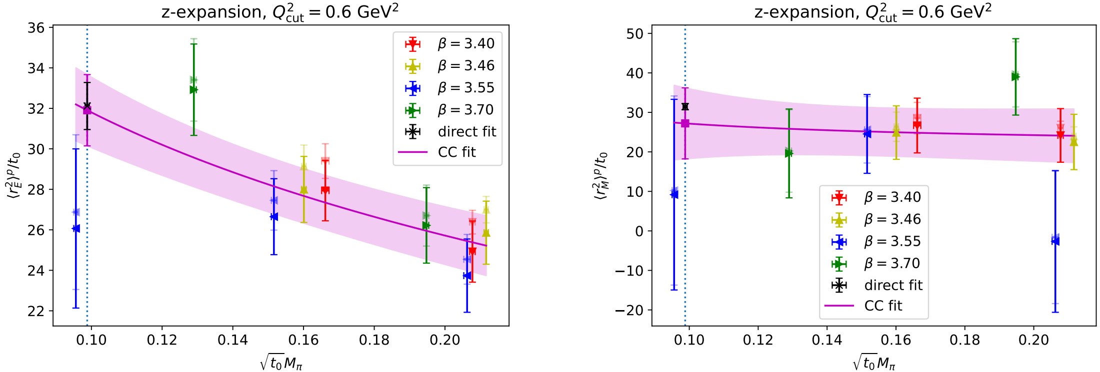

- Good agreement with direct fits, albeit with significantly larger errors
- Not sufficiently stable against fluctuations on single momenta or ensembles

Crosscheck of direct fits with z-expansion: proton magnetic moment

Significantly smaller than direct fits, which are compatible with experiment

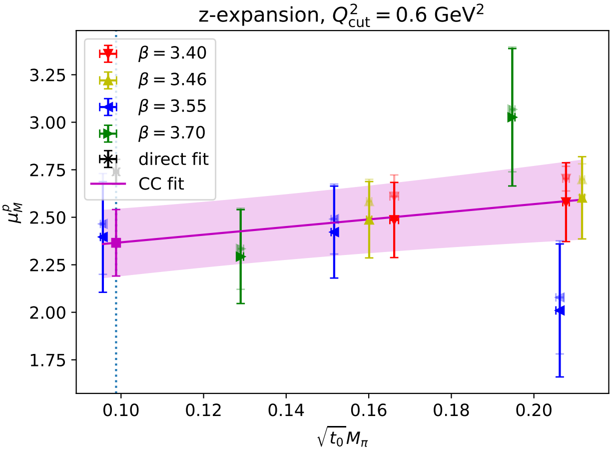

Zemach integrand

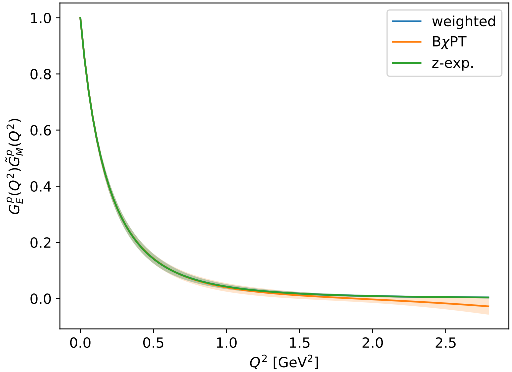

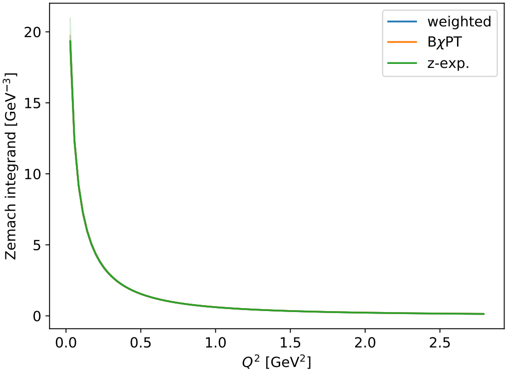

- z-expansion agrees very well with BχPT parametrization in the region where it is fitted
- For the integration, smoothly replace the BχPT parametrization by the z-expansion